ARTICLE

doi:10.1038/nature11406

Bose glass and Mott glass of quasiparticles in a doped quantum magnet

Rong Yu[1], Liang Yin[2], Neil S. Sullivan[2], J. S. Xia[2], Chao Huan[2], Armando Paduan-Filho[3], Nei F. Oliveira Jr[3], Stephan Haas[4], Alexander Steppke[5], Corneliu F. Miclea[6,7], Franziska Weickert[6], Roman Movshovich[6], Eun-Deok Mun[6], Brian L. Scott[6], Vivien S. Zapf[6] & Tommaso Roscilde[8]

The low-temperature states of bosonic fluids exhibit fundamental quantum effects at the macroscopic scale: the best-known examples are Bose–Einstein condensation and superfluidity, which have been tested experimentally in a variety of different systems. When bosons interact, disorder can destroy condensation, leading to a 'Bose glass'. This phase has been very elusive in experiments owing to the absence of any broken symmetry and to the simultaneous absence of a finite energy gap in the spectrum. Here we report the observation of a Bose glass of field-induced magnetic quasiparticles in a doped quantum magnet (bromine-doped dichloro-tetrakis-thiourea-nickel, DTN). The physics of DTN in a magnetic field is equivalent to that of a lattice gas of bosons in the grand canonical ensemble; bromine doping introduces disorder into the hopping and interaction strength of the bosons, leading to their localization into a Bose glass down to zero field, where it becomes an incompressible Mott glass. The transition from the Bose glass (corresponding to a gapless spin liquid) to the Bose–Einstein condensate (corresponding to a magnetically ordered phase) is marked by a universal exponent that governs the scaling of the critical temperature with the applied field, in excellent agreement with theoretical predictions. Our study represents a quantitative experimental account of the universal features of disordered bosons in the grand canonical ensemble.

Disorder can have a very strong effect on quantum fluids. Owing to their wave-like nature, quantum particles are subject to interference when scattering against disordered potentials. This leads to their quantum localization (or Anderson localization), which prevents—for example—electrons from conducting electrical currents in strongly disordered metals[1], and non-interacting bosons from condensing into a zero-momentum state[2]. Yet interacting bosons represent a matter wave with arbitrarily strong nonlinearity, whose localization properties in a random environment cannot be deduced from the standard theory of Anderson localization. It has been predicted[3,4] that for strongly interacting bosons, Anderson localization manifests itself in the Bose glass: in this phase, the collective modes of the system—and not the individual particles—are Anderson-localized over arbitrarily large regions, leading to a gapless energy spectrum, and a finite compressibility of the fluid. Moreover, nonlinear bosonic matter waves should undergo a localization–delocalization quantum phase transition in any spatial dimension when the interaction strength is varied[3,4]; the transition brings the system from a non-interacting Anderson insulator to an interacting superfluid condensate, or from a superfluid to a Bose glass. Such a transition is relevant for a large variety of physical systems, including superfluid helium in porous media[5], Cooper pairs in disordered superconductors[6,7], and cold atoms in random optical potentials[8,9]. Despite the long history of activity on the subject, a quantitative understanding of the phase diagram of disordered and interacting bosons based on experiments is still lacking.

Recent experiments have demonstrated the capability of realizing and controlling novel Bose fluids made of quasiparticles in condensed matter systems (ref. 9 and 10, and references therein). In this context, a prominent place is occupied by the equilibrium Bose fluid realized in quantum magnets subjected to a magnetic field (ref. 10, and references therein) in which disorder can be introduced in a controlled way by chemical doping, leading to novel bosonic phases[10–13]. The ground state of such systems without disorder and in zero field corresponds to a gapped bosonic Mott insulator. Extra bosons can be injected into the system by applying a critical magnetic field that overcomes the gap, and that drives a transition to a superfluid state (a magnetic Bose–Einstein condensate, BEC). Such a state corresponds to an XY antiferromagnetic state of the spin components transverse to the field. Here we investigate the Bose fluid of magnetic quasiparticles realized in the model compound $NiCl_2{\cdot}4SC(NH_2)_2$ (DTN)[10] with spin $S = 1$ via experiments (a.c. magnetic susceptibility, d.c. magnetization and specific heat), and large-scale quantum Monte Carlo (QMC) simulations. Disorder is introduced by Cl → Br substitution, which, as we will see, leads to randomness in the bosonic hoppings and interactions. We select this compound because the parent compound (pure DTN) has been shown to exhibit Bose–Einstein condensation of the spin system with high accuracy[17]. We also select it because it can be doped very cleanly, which is extremely unusual among similar quantum magnets. The Cl atom sits in an over-sized cage such that it can be replaced by a larger Br atom with very minimal changes in the lattice constants and no observable structural distortion (see Supplementary Information). Thus we can use Br substitution to modify bosonic parameters (for example, magnetic exchange and crystalline electric fields) without other unwanted effects, such as local changes in site symmetry and local modulations of the lattice constant. In experiments and QMC simulations, we observe a Bose glass in two extended regions of the temperature–magnetic field phase diagram of Br-doped DTN. The gapless nature of the Bose glass manifests itself in a finite uniform magnetic susceptibility (corresponding to the compressibility of the quasiparticles), and in a non-exponential decay of the specific heat at low temperature, probing the low-energy density of states. This gapless state extends down to zero field: in this limit the compressibility/susceptibility vanishes while the spectrum remains gapless, giving rise to a Mott glass[18–21]. We investigate the thermodynamic signatures of the Mott and Bose glasses, and the Bose-glass-to-superfluid transition, which is characterized by a novel universal exponent for the scaling of the condensation temperature with applied field.

[1]Department of Physics and Astronomy, Rice University, Houston, Texas 77005, USA. [2]Department of Physics and National High Magnetic Field Laboratory, University of Florida, Gainesville, Florida 32611, USA. [3]Instituto de Física, Universidade de São Paulo, 05315-970 São Paulo, Brazil. [4]Department of Physics and Astronomy, University of Southern California, Los Angeles, California 90089-0484, USA. [5]Max Planck Institute for Chemical Physics of Solids, Nöthnitzer Strasse 40, 01187 Dresden, Germany. [6]Condensed Matter and Magnet Science, Los Alamos National Laboratory, Los Alamos, New Mexico 87545, USA. [7]National Institute for Materials Physics, 077125 Bucharest-Magurele, Romania. [8]Laboratoire de Physique, Ecole Normale Supérieure de Lyon, CNRS UMR5672, 46 Allée d'Italie, 69364 Lyon, France.

Magnetic properties of pure DTN

The magnetic properties of pure DTN are those of antiferromagnetic $S = 1$ chains of Ni^{2+} ions, oriented along the crystallographic c axis, and coupled transversely in the a–b plane[16,22]. (The structure of DTN is actually that of two interpenetrating tetragonal lattices, which can be considered effectively as decoupled[23]). The magnetic Hamiltonian is given by

$$\mathcal{H} = J_c \sum_{\langle ij \rangle_c} S_i \cdot S_j + J_{ab} \sum_{\langle ln \rangle_{ab}} S_l \cdot S_n + D \sum_i \left(S_i^z\right)^2 - g\mu_B H \sum_i S_i^z \quad (1)$$

where $S_i = (S_i^x, S_i^y, S_i^z)$ is the spin operator at site i, $J_c = 2.2$ K is the antiferromagnetic coupling for bonds $\langle ij \rangle$, along the c axis, $J_{ab} = 0.18$ K is the coupling for bonds $\langle lm \rangle_{ab}$ in the a–b plane, and $D = 8.9$ K is the single-ion anisotropy. μ_B is the Bohr magneton, g is the gyromagnetic factor along the c axis, and H is the applied magnetic field. Here we use a value $g = 2.31$ which is larger by 2% with respect to the value quoted in ref. 22. This value allows us to obtain the best agreement between the experimental and theoretical magnetization curves. In zero field, the large D forces the system into a quantum paramagnetic state with each spin close to its $|m_S = 0\rangle$ state (m_S being the S^z eigenvalue). Mapping the $S = 1$ spin states onto bosonic states with occupation $n = m_S + 1$, the quantum paramagnet corresponds to a Mott insulator of bosons with $n = 1$ particles per Ni site, and with a gap $\Delta \approx D - 2J_c - 4J_{ab} + \mathcal{O}(J_i^2/D)$ for the addition of an extra boson.

A magnetic field exceeding the value $H_{c1}^{(0)} = \Delta/g\mu_B \approx 2.1$ T is able to close the spin gap and to create a finite density of excess bosons that condense into a magnetic BEC (see Fig. 1a). The appearance of excess bosons translates into a finite magnetization along the field axis; their long-range phase coherence translates into long-range XY antiferromagnetic order transverse to the field. Long-range order persists up to a critical condensation temperature T_c which, for $H \gtrsim H_{c1}^{(0)}$, scales with the applied field as $T_c \propto \left|H - H_{c1}^{(0)}\right|^{\phi}$. Here $\phi = 2/3$, as predicted by mean-field theory for a diluted gas of excess bosons, and as measured with very high accuracy down to 1 mK (ref. 17). When the magnetic field is increased further, the spins are brought to saturation for $H = H_{c2}^{(0)} = (D + 4J_c + 8J_{ab})/g\mu_B = 12.3$ T, and the system transitions from a BEC to a Mott insulator with $n = 2$ particles per site. Correspondingly, the BEC critical temperature vanishes as $T_c \propto \left|H - H_{c2}^{(0)}\right|^{\phi}$.

Experimental phase diagram of Br-doped DTN

We have measured the critical temperatures and fields for magnetic Bose–Einstein condensation in $Ni(Cl_{1-x}Br_x)_2{\cdot}4SC(NH_2)_2$ (referred to as Br-DTN) with $x = 0.08 \pm 0.005$ by measuring the a.c. susceptibility at low frequencies and the specific heat (see Supplementary Information). Measurements of a.c. and d.c. susceptibility were performed at fixed temperature and varying fields, and they show a step-like increase/decrease corresponding to the critical field for Bose–Einstein condensation, similar to the pure sample[17,24] (see Fig. 2a and b). The main difference compared to pure DTN is that—at low temperatures—the upper and lower edge of the steps are rounded by disorder; as we will see below, this rounding is a fundamental indication of the nature of the phases connected by the transition. An independent estimate of the critical Bose–Einstein condensation temperature as a function of the field is obtained by the location of a sharp λ-peak in the specific heat (Fig. 2c). The remarkable sharpness of the features in the specific heat corresponding to the BEC transition supports the fact that true long-range order persists despite the strong doping introduced in the system. Moreover, for temperatures below the λ-peak the specific heat clearly follows a T^{ϕ} behaviour, consistent with long-range XY antiferromagnetic order in three dimensions.

Figure 3 summarizes the experimental phase diagram of Br-DTN. Br doping has a profound affect on the phase diagram of DTN: in particular both the lower and upper critical fields for the onset of magnetic Bose–Einstein condensation at $T \to 0$ are found to shift to lower values, $H_{c1} = 1.07(1)$ T and $H_{c2} = 12.16(1)$ T, as shown in Fig. 3. But most importantly the magnetic behaviour of Br-DTN

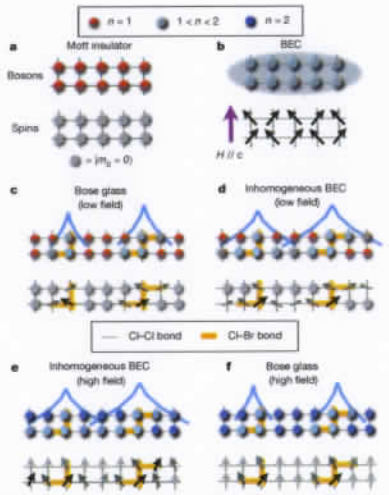

Figure 1 | Sketch of the bosonic phases of DTN and Br-doped DTN. In the undoped case, an increasing magnetic field along the c axis (purple arrow) drives the system from a Mott insulating phase (**a**) to a BEC phase (**b**) by injecting delocalized excess bosons (indicated in cyan) on top of the Mott insulating background at density $n = 1$. In the doped case, an arbitrarily weak magnetic field can inject extra bosons in the rare Br-rich regions (indicated by the orange bonds) which are localized and incoherent in the (low-field) Bose glass phase (**c**)—their localized wavefunction is sketched by the light-blue lines, and the corresponding local orientations of the spins are sketched by the arrows (the darker the arrow, the larger the fluctuating transverse moment induced by the field). Further increasing the magnetic field leads to the percolation of phase coherence via coherent tunnelling of the excess bosons between the localized regions, giving rise to an inhomogeneous BEC (**d**). For strong magnetic fields $H \lesssim H_{c2}$ the spins away from the Br-bonds are close to saturation/double occupancy (represented in dark blue), and unpolarized spins/singly occupied sites, corresponding to bosonic holes, only survive in the Br-rich regions (**e**). These holes are localized into disconnected, mutually incoherent states when entering the high-field Bose glass (**f**).

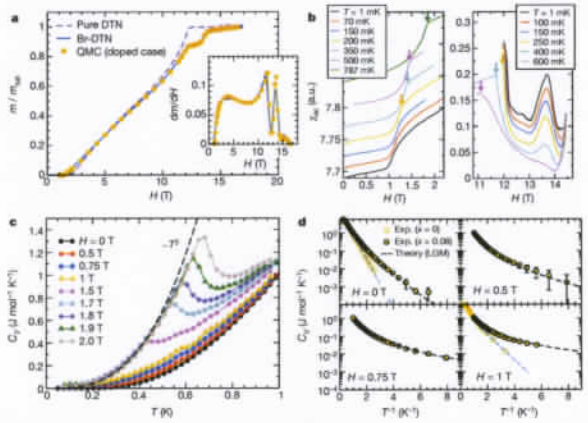

Figure 2 | Thermodynamic properties of the magnetic Bose glass and BEC phases. **a**, Magnetization curve of Br-DTN at $T = 19$ mK, compared to QMC results, and to pure DTN magnetization (measured at $T = 16$ mK). Inset, the d.c. susceptibility curve, obtained by differentiating the magnetization. **b**, a.c. susceptibility of Br-DTN at frequency $f = 88.7$ Hz close to the lower and upper critical fields. The curves have been shifted with respect to one another for readability purposes. The arrows indicate the appearance of sharp kinks at higher temperatures. **c**, Specific heat of Br-DTN from $H = 0$ T to $H = 2$ T. **d**, Specific heat of Br-DTN in the Mott glass and Bose glass phases for $H \leq H_{c1} \approx 1$ T, showing a non-exponential decay as $T \to 0$; a comparison is made to the predictions of theory based on the local-gap model (LGM), and to the data for pure DTN; in the upper-left and lower-right panels, the blue dashed line is a fit of the pure-DTN data to $A\exp(-\Delta(H)/k_BT)$, where A is a constant and $\Delta(H)/k_B = g\mu_B\left(H_{c1}^{(0)} - H\right)/k_B = 3.16$ K for $H = 0$ and 1.64 K for $H = 1$ T. Error bars, 1 s.d.

outside the BEC region is completely different to that of the pure system. In the pure system, the ground state outside the magnetic BEC is a Mott insulator with a large spin gap Δ away from the critical fields. This leads to an exponential suppression of the specific heat C_V at low temperatures $k_BT \lesssim \Delta$ as $C_V \propto \exp[-\Delta/(k_BT)]$, as shown in Fig. 2d, and to a similarly vanishing susceptibility for $T \to 0$. On the contrary, for $x = 0.08$, we observe that the susceptibility is finite for $H \geq H_{c1}$, and it even exhibits a strong satellite peak for $H \approx 13.5$ T. The susceptibility vanishes only for $H = H_s \approx 17$ T, corresponding to the saturation field of the entire sample, which is pushed to a much higher value than in the pure sample (where $H_s = H_{c2}^{(0)} = 12.6$ T). In the region $H \leq H_{c1}$ we observe that the specific heat exhibits a non-exponential decay, down to zero field (Fig. 2d). Therefore we can conclude that the non-magnetic phases for $0 \leq H \leq H_s$ correspond to gapless bosonic insulators, which, as we will see, can be identified with a compressible Bose glass (for $H > 0$) and an incompressible Mott glass (for $H = 0$).

Modelling Br doping

Br-DTN can be successfully modelled theoretically by considering that Br substitution for Cl affects the super-exchange paths associated with the J_c couplings, and it also affects the crystal field locally owing to the larger atomic radius of Br with respect to Cl. The disappearance of the spin gap down to $H = 0$ and the upward shift of the saturation field suggests that Br doping locally strengthens the magnetic coupling J_c and lowers the anisotropy D. For simplicity, we only consider that Ni–Cl–Cl–Ni bonds in DTN can be turned into Ni–Cl–Br–Ni or Ni–Br–Cl–Ni, and we neglect Ni–Br–Br–Ni bonds that represent only 0.6% of the total bonds for $x = 0.08$.

We assign a J_c' value to the magnetic exchange coupling of the Br-doped bonds, and a D' value to the single-ion anisotropies of the Ni ion adjacent to the Br dopant. Note that for a doping concentration x, we have a fraction $2x$ of doped bonds, given that each bond can accommodate a Br dopant on two different Cl sites. We then use J_c' and D' as fitting parameters of the full low-temperature magnetization curve in Fig. 2a, which is calculated using QMC simulations (see Supplementary Information). We find an extremely good agreement between experimental data and simulation for $J_c' \approx 2.35 J_c$ and $D' \approx D/2$, giving us confidence that we are able to quantitatively model the fundamental microscopic effects of doping in Br-DTN. Indeed, the critical temperature for Bose–Einstein condensation, extracted from a finite-size scaling analysis of the simulation data with doping $x = 0.075$ (see Supplementary Information), is in

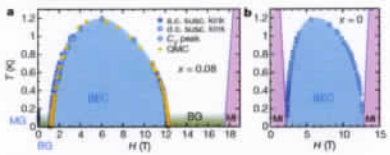

Figure 3 | Phase diagrams in the field–temperature plane. **a**, Experimental phase diagram of Br-doped DTN from specific heat and susceptometry, compared to QMC data. The following phases are represented: Bose–Einstein condensate (BEC), Bose glass (BG) and Mott glass (MG). The lilac regions represent the magnitude of the spin gap in the Mott insulating (MI) phase. **b**, Experimental phase diagram of pure DTN (based on specific heat and the magnetocaloric effect[23]).

remarkable quantitative agreement with the experiment, as shown in Fig. 3a. The critical fields estimated from simulations are $H_{c1} = 1.172(5)$ T and $H_{c2} = 12.302(5)$ T, slightly larger (by ~0.1 T and 0.14 T, respectively) than the experimental values. However the large downward shift of H_{c1} (by about 1 T) with respect to the pure system is correctly captured. In the following we discuss the main features of the Bose glass and Mott glass phases expected for the model of Br-DTN, and corroborate such expectations quantitatively with the experimental data.

Bose and Mott glasses

The results of our experiments on Br-DTN are consistent with a Bose glass for certain applied magnetic fields, and also with a Mott glass for $H = 0$ (see Fig. 3). A Mott glass has the peculiar property of being incompressible—that is, it has a vanishing susceptibility at $T = 0$, despite being gapless[19–21] (see also Supplementary Information). Br-DTN represents to our knowledge the first experimental realization of a Mott glass. To understand how the Mott glass applies to Br-DTN, consider that a compound in which all c-axis bonds contain a Br dopant (leading to couplings J_c' everywhere, and to an anisotropy D' on one of the two sites connected by the bond) will be a BEC even in zero field (see Supplementary Information). This means that rare Br-rich regions in Br-DTN behave locally as mini-BECs, and hence they are locally gapless. Strictly speaking, Br-rich regions will have a residual gap owing to their finite size. However, the statistical distribution of sizes has no upper bound, so that the distribution of local gaps has no lower bound, and consequently Br-DTN is globally gapless even in zero field. The corresponding bosonic phase is therefore a gapless insulator with spin inversion symmetry along the field axis, a commensurate boson density $n = 1$, and a vanishing compressibility resulting from the above symmetry[20]. As soon as a magnetic field is applied to this Mott glass, excess bosons are injected, which Anderson-localize around the rare Br-rich regions, resulting in a Bose glass (Fig. 1c). In the spin language, spins in the Br-rich regions acquire a finite magnetization along the field, and their transverse components correlate antiferromagnetically over a finite range, but the local phase of the antiferromagnetic order is different from region to region so that the system remains globally paramagnetic. Long-range phase coherence of the local order parameters—corresponding to the local phases of the bosonic wavefunction—is established only when the localized states of the bosons grow enough under the action of the applied field to overlap, leading to coherent tunnelling of bosons between neighbouring localized states (Fig. 1d). The resulting phase is a highly inhomogeneous BEC[26].

We can quantitatively test the picture of bosons localized in rare Br-rich regions against the thermodynamic behaviour of Br-DTN by using a simplified local-gap model (LGM). Within this model (see Supplementary Information), the low-temperature and low-field behaviour of the system is reduced to that of a collection of three-level systems, corresponding to a local longitudinal magnetization $m_{z,\mathrm{loc}} = 0, \pm 1$ for each localized state. There is a finite-size gap $\Delta_N \approx c/N$ (for zero field) between the $m_{z,\mathrm{loc}} = 0$ ground state and the $m_{z,\mathrm{loc}} = \pm 1$ excited states, where N is the number of sites in the Br-rich cluster and c is a fitting parameter. The low-temperature specific heat in zero field can then be predicted analytically to be

$$C_V(T) \propto t^{-5/4} \exp\left(-2\sqrt{cx_0/t}\right) \qquad (2)$$

where $t = k_BT/J_c$ and $x_0 = \log(2x)$; this expression displays a stretched exponential behaviour that uniquely characterizes the Mott glass[21]. The c parameter, and an overall prefactor, are used as fitting parameters of the experimental data in zero field, leading to an extremely good fit, as shown in Figs 2d and 4. Notably, no further adjustable parameters are necessary to fit the finite-field data, displayed in Fig. 2d, which also show a remarkable agreement with the theory prediction up to $H \approx H_{c1}$.

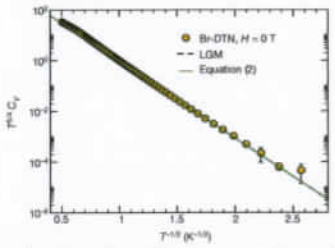

Figure 4 | Specific heat scaling and Mott glass. The specific heat in zero field is seen to display the characteristic Mott glass scaling at low temperatures, $\exp(-T^{-1/2})$. The solid lines are theoretical predictions based on the numerical solution of the local gap model (LGM) and its approximate analytical solution given by equation (2), with parameter $c = 3.02$. Error bars, 1 s.d.

High-field Bose glass

For $H \to H_{c2}$ the magnetization approaches the value $m_z = 1 - 2x \approx 0.84$, where all spins not connected to a Br-doped bond are polarized—and indeed H_{c2} lies very close to the polarization field $H_{c2}^{(0)}$ of pure DTN. The full polarization of the Br-poor regions leads to a pseudo-plateau in the magnetization at $m \approx m_s$ (pseudo because it still exhibits a small finite slope—a similar feature has also been observed in a Br-doped spin ladder at high field[11]). We interpret this feature as corresponding to the high-field Bose glass, which is characterized by the localization of bosonic holes, or singly occupied sites with $m_S = 0$, in a background of doubly occupied sites with $m_S = 1$ (Fig. 1f). The magnetically disordered nature of the high-field Bose glass phase could only be inferred from the susceptibility data and from our numerics. Indeed, in the experiments we could not determine unambiguously the absence of a λ-anomaly in the specific heat at low temperatures for $H \approx H_{c2}$, given that at such high fields the low-temperature specific heat of DTN is dominated by a Schottky anomaly whose origin can be ascribed to nuclear spins[27]. The localized bosonic holes persist up to the saturation field H_s, which is roughly the field necessary to fully polarize a homogeneous system with J_c' couplings and D' anisotropies everywhere. The step-like feature in the magnetization at the upper bound of the pseudo-plateau is therefore induced by the saturation of the Br-rich clusters, and it is smeared owing to the fact that such clusters have random geometries and therefore a distribution of local saturation fields, with an upper bound of H_s. One might suspect that the peak anomaly in the susceptibility corresponding to the step feature in the magnetization is associated with a further transition, but the numerical data, showing the same anomaly, allow us to conclude that the ground state is disordered in that field range.

Thermal percolation crossover

The physics described so far is valid only for very low temperatures. As the temperature is increased (above ~200 mK, as we will see below), the bosons that were localized in the Bose glass state are expected to thermally delocalize and proliferate. This leads to a thermal percolation of their density profile (corresponding to the longitudinal magnetization profile) throughout the sample[26]. Thus a more ordinary paramagnetic state is expected to appear at higher temperatures, and the nature of the field-driven transition into the BEC phase should also change fundamentally. Indeed, at temperatures below the thermal percolation crossover, the BEC transition should occur as sketched in Fig. 1c–f, by coherent tunnelling of bosons between localized states, resulting in a highly inhomogeneous BEC phase. This picture changes above the thermal percolation crossover. Now in the normal phase, the bosons move incoherently on a pre-percolated network of magnetized sites,

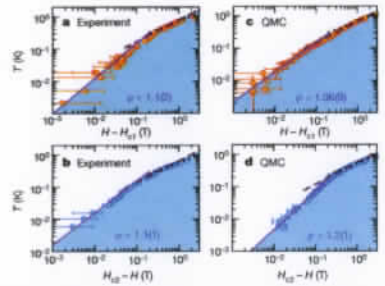

Figure 5 | Critical temperature scaling close to the zero-temperature critical fields. The scaling of the critical temperature with the distance from the $T = 0$ critical fields exhibits a crossover between various exponents. The dashed and dotted lines indicate a fit to the form $a|H - H_{c1(2)}|^{2/3}$ and $a|H - H_{c1(2)}|^{1/2}$ respectively, while the solid line is a fit to $a'|H - H_{c1(2)}|^{\phi}$, with the resulting ϕ exponent indicated in the figure (a and a' are fitting parameters). **a**, **b**, The critical line extracted from the a.c. susceptibility; **c**, **d**, the critical line obtained from the QMC simulations. Error bars, 1 s.d.

and their BEC transition upon increasing the field corresponds therefore to condensation on a random three-dimensional percolated lattice, which is fully analogous to condensation on a regular three-dimensional lattice. Signatures of the thermal percolation crossover can be found in the critical behaviour of the a.c. susceptibility: at low temperatures ($T \lesssim 200$ mK) it exhibits a rounded shoulder for $H \gtrsim H_{c1}$ and $H \lesssim H_{c2}$, and at higher temperatures it shows a sharp kink—analogous to what is observed in the pure system[17,24] (see Fig. 2b).

But the most marked signature of the thermal percolation crossover is observed in the scaling of the critical temperature with the applied field, shown in Fig. 5. Plotting T_c versus $|H - H_{c1(2)}|$ on a log–log scale (Fig. 5a, b), we clearly observe a kink separating two different scaling regimes. At high temperatures, ($T \gtrsim 200 - 300$ mK) the field-dependence of T_c is essentially consistent with a pure-system scaling for low temperatures, $T_c \propto |H - H_{c1(2)}|^{\phi}$ with $\phi = 2/3$, or with a pure-system scaling for intermediate temperatures with $\phi = 1/2$, as observed in other magnetic BEC systems[29]. At low temperatures, the scaling exponent crosses over to novel values, $\phi = 1.1(2)$ (close to H_{c1}) and $\phi = 1.1(1)$ (close to H_{c2}), which are consistent within the error (see Supplementary Information for a discussion of the estimate of ϕ). Moreover, these scaling exponents are also consistent with the values extracted from our QMC simulations (Fig. 5c, d; $\phi = 1.06(9)$ and $1.2(1)$ close to H_{c1} and H_{c2} respectively). Simulations also show a rough quantitative agreement for the crossover temperature range. Most remarkably, a consistent value of the exponent ϕ at low temperature is also observed theoretically for the magnetic Hamiltonian of DTN subject to a different type of disorder, namely site dilution[29]. We can therefore conclude that the low-temperature scaling of T_c exhibits an exponent $\phi \approx 1$–1.1 which is a universal feature of the Bose glass–BEC transition. Its value deviates from the prediction $\phi > 2$ of ref. 4, but this prediction is based on a scaling Ansatz for the free energy close to the quantum critical point which is found to be inconsistent with other observations on Br-DTN, as well as with numerical simulations[29]. Therefore we conclude that our results call for a generalization of the scaling assumptions for the disordered-boson quantum critical point.

Conclusions

We have performed a comprehensive experimental and theoretical study of the disordered and strongly interacting Bose fluid realized in a doped quantum magnet (Br-DTN) under application of a magnetic field. We provide substantial evidence for the existence of gapless insulating phases of the bosons—the Mott glass and the Bose glass—and we investigate the quantitative features associated with their thermodynamic behaviour. These phases can be quantitatively described as a Bose fluid fragmented over an extensive number of localized states with variable local gaps, dominating the response of the system. The presence of a Bose glass leads to a novel and seemingly universal exponent governing the scaling of the critical temperature for the transition from Bose glass to BEC. The remarkable agreement between theory and experiment shows that Br-DTN is an extremely well controlled realization of a disordered Bose fluid, which allows a detailed experimental study of the thermal phase diagram of disordered bosons in the grand-canonical ensemble.

METHODS SUMMARY

Br-DTN crystals were prepared at the University of São Paulo, and their X-ray analysis was performed at the Los Alamos National Laboratories. The same crystal was used for a.c. susceptibility and specific heat measurements—the specific heat sample was a small slice of the a.c. susceptibility sample. All measurements were made with the magnetic field applied along the tetragonal axis (c axis) of the sample. The a.c. susceptibility measurements were carried out using a PrNi$_5$ nuclear refrigerator (down to 1 mK) and a 15 T magnet at the High B/T facility of the National High Magnetic Field Laboratory in Gainesville. The field sweep rates were adjusted to values as low as 10^{-4} T min^{-1} to guarantee the full relaxation of the sample at the lowest temperatures probed. The d.c. magnetization was measured at the University of São Paulo by using a dilution refrigerator at 19 mK. Specific heat was measured in a Quantum Design ^{3}He/^{4}He dilution refrigerator down to 50 mK using the thermal relaxation method. The numerical simulations were based on the stochastic series expansion approach with directed-loop updates, and they were performed on the Jaguar cluster of the National Center for Computational Sciences (Oak Ridge National Laboratories).

Received 14 May; accepted 11 July 2012.

1. Kramer, B. & MacKinnon, A. Localization: theory and experiment. *Rep. Prog. Phys.* **56,** 1469–1564 (1993).
2. Fallani, L., Fort, C. & Inguscio, M. Bose-Einstein condensates in disordered potentials. *Adv. At. Mol. Opt. Phys.* **56,** 119–160 (2008).
3. Giamarchi, T. & Schulz, H. J. Anderson localization and interactions in one-dimensional metals. *Phys. Rev. B* **37,** 325–340 (1988).
4. Fisher, M. P. A., Weichman, P. B., Grinstein, G. & Fisher, D. S. Boson localization and the superfluid-insulator transition. *Phys. Rev. B* **40,** 546–570 (1989).
5. Crowell, P. A., Van Keuls, F. W. & Reppy, J. D. Onset of superfluidity in ^{4}He films adsorbed on disordered substrates. *Phys. Rev. B* **55,** 12620–12634 (1997).
6. Sacépé, B. *et al.* Localization of preformed Cooper pairs in disordered superconductor. *Nature Phys.* **7,** 239–244 (2011).
7. Bouadim, K., Loh, Y. L., Randeria, M. & Trivedi, N. Single- and two-particle energy gaps across the disorder-driven superconductor-insulator transition. *Nature Phys.* **7,** 884–889 (2011).
8. Sanchez-Palencia, L. & Lewenstein, M. Disordered quantum gases under control. *Nature Phys.* **6,** 87–95 (2010).
9. Deng, H. Haug, H. & Yamamoto, Y. Exciton-polariton Bose-Einstein condensation. *Rev. Mod. Phys.* **82,** 1489–1537 (2010).
10. Giamarchi, T., Rüegg, Ch. & Tchernyshyov, O. Bose-Einstein condensation in magnetic insulators. *Nature Phys.* **4,** 198–204 (2008).
11. Nohadani, O., Wessel, S. & Haas, S. Bose-glass phases in disordered quantum magnets. *Phys. Rev. Lett.* **95,** 227201 (2005).
12. Roscilde, T. & Haas, S. Quantum localization in bilayer Heisenberg antiferromagnets with site dilution. *Phys. Rev. Lett.* **95,** 207206 (2005).
13. Roscilde, T. Field-induced quantum-disordered phases in S= 1/2 weakly coupled dimer systems with site dilution. *Phys. Rev. B* **74,** 144418 (2006).
14. Manaka, H., Kolomiets, A. V. & Goto, T. Disordered states in (PA-Cu(Cl)$_x$Br$_{1-x}$)$_3$ induced by bond randomness. *Phys. Rev. Lett.* **101,** 077204 (2008).
15. Hong, T., Zheludev, A., Manaka, H. & Regnault, L.-P. Evidence of a magnetic Bose glass in $(CH_3)_2CHNH_3Cu(Cl_{0.95}Br_{0.05})_3$ from neutron diffraction. *Phys. Rev. B* **81,** 060410 (2010).
16. Zapf, V. S. *et al.* Bose-Einstein condensation of S = 1 nickel spin degrees of freedom in NiCl$_2$-4SC(NH$_2$)$_2$. *Phys. Rev. Lett.* **96,** 077204 (2006).
17. Yin, L., Xia, J. S., Zapf, V. S., Sullivan, N. S. & Paduan-Filho, A. Direct measurement of the Bose-Einstein condensation universality class in NiCl$_2$-4SC(NH$_2$)$_2$ at ultralow temperatures. *Phys. Rev. Lett.* **101,** 187205 (2008).
18. Orignac, E., Giamarchi, T. & Le Doussal, P. A possible new phase of commensurate insulators with disorder: the Mott glass. *Phys. Rev. Lett.* **83,** 2378–2381 (1999).
19. Prokof'ev, N. & Svistunov, B. Superfluid-insulator transition in commensurate disordered bosonic systems: large-scale worm algorithm simulations. *Phys. Rev. Lett.* **92,** 015703 (2004).
20. Altman, E., Kafri, Y., Polkovnikov, A. & Refael, G. Phase transition in a system of one-dimensional bosons with strong disorder. *Phys. Rev. Lett.* **93,** 150402 (2004).

21. Roscilde, T. & Haas, S. Mott glass in site-diluted S=1 antiferromagnets with single-ion anisotropy. *Phys. Rev. Lett.* **99,** 047205 (2007).
22. Zvyagin, S. A. *et al.* Magnetic excitations in the spin-1 anisotropic Heisenberg antiferromagnetic chain system NiCl$_2$-4SC(NH$_2$)$_2$. *Phys. Rev. Lett.* **98,** 047205 (2007).
23. Zvyagin, S. A. *et al.* Spin dynamics of NiCl$_2$-4SC(NH$_2$)$_2$ in the field-induced ordered phase. *Phys. Rev. B* **77,** 092413 (2008).
24. Yin, L., Xia, J. S., Zapf, V. S., Sullivan, N. S. & Paduan-Filho, A. Magnetic susceptibility measurements at ultra-low temperatures. *J. Low Temp. Phys.* **158,** 710–715 (2010).
25. Balabanyan, K. G., Prokof'ev, N. & Svistunov, B. Superfluid-insulator transition in commensurate one-dimensional bosonic system with off-diagonal disorder. *Phys. Rev. Lett.* **95,** 055701 (2005).
26. Yu, R., Haas, S. & Roscilde, T. Universal phase diagram of disordered bosons from a doped quantum magnet. *Europhys. Lett.* **89,** 10009 (2010).
27. Weickert, F. *et al.* Low temperature thermodynamic properties near the field-induced quantum critical point in DTN. *Phys. Rev. B* **85,** 184408 (2012).
28. Kawashima, N. Quantum critical point of the *XY* model and condensation of field-induced quasiparticles in dimer compounds. *J. Phys. Soc. Jpn* **73,** 3219–3222 (2004).
29. Yu, R. *et al.* Quantum critical scaling at a Bose-glass/superfluid transition: theory and experiment on a model quantum magnet. Preprint at http://arXiv.org/abs/1204.5409 (2012).

Supplementary Information is available in the online version of the paper.

Acknowledgements Work at the High Magnetic Field Laboratory at the Physics Institute of the University of São Paulo was supported in part by the Brazilian agencies FAPESP and CNPq. Measurements at the NHMFL High B/T and pulsed field facilities were supported by NSF grant DMR 0654118, by the State of Florida, and by the DOE. Work at LANL was supported by the NSF, and by the DOE's Laboratory Directed Research and Development programme under 20100043DR. C.F.M. acknowledges support by UEFISCDI (project RP-10). The numerical simulations were performed on the computer facilities of the NCCS at the Oak Ridge National Laboratories, and supported by INCITE Award MAT013 of the Office of Science, DOE. Further theory work was supported by the DOE (grant DE-FG03-01ER45908 and DE-FG02-05ER46240), the NSF (grant DMR-1006985) and by the Robert A. Welch Foundation (grant C-1411).

Author Contributions R.Y., S.H. and T.R. performed the numerical simulations and the theoretical analysis; L.Y., N.S.S., J.S.X. and C.H. performed the susceptibility measurements; A.P.-F. and N.F.O. synthesized the samples and performed the d.c. magnetization measurements; A.S., C.F.M., F.W., R.M., E.-D.M. and V.S.Z. performed the specific heat measurements; and B.L.S. performed the X-ray measurements. V.S.Z. coordinated the experimental efforts and T.R. the theoretical ones. T.R. wrote the manuscript, with the contributions of all the authors.

Author Information Reprints and permissions information is available at www.nature.com/reprints. The authors declare no competing financial interests. Readers are welcome to comment on the online version of the paper. Correspondence and requests for materials should be addressed to T.R. (tommaso.roscilde@ens-lyon.fr).